

Composition and fate of short-period super-Earths

The case of CoRoT-7b

D. Valencia¹, M. Ikoma^{1,2}, T. Guillot¹, and N. Nettelmann³

¹ Observatoire de la Côte d’Azur, Université de Nice-Sophia Antipolis, CNRS UMR 6202, BP 4229, F-06304 Nice Cedex 4, France

² Dept. of Earth and Planetary Sciences, Tokyo Institute of Technology, Ookayama, Meguro-ku, Tokyo 152-8551, Japan

³ Institut für Physik, Universität Rostock, D-18051 Rostock, Germany

Preprint online version: November 12, 2018

ABSTRACT

Context. The discovery of CoRoT-7b, a planet of radius $1.68 \pm 0.09 R_{\oplus}$, mass $4.8 \pm 0.8 M_{\oplus}$ and orbital period of 0.854 days demonstrates that small planets can orbit extremely close to their star.

Aims. Several questions arise concerning this planet, in particular concerning its possible composition, and fate.

Methods. We use knowledge of hot Jupiters, mass loss estimates and models for the interior structure and evolution of planets to understand its composition, structure and evolution.

Results. The inferred mass and radius of CoRoT-7b are consistent with a rocky planet that would be significantly depleted in iron relative to the Earth. However, a one sigma increase in mass ($5.6 M_{\oplus}$) and one sigma decrease in size ($1.59 R_{\oplus}$) would make the planet compatible with an Earth-like composition (33% iron, 67% silicates). Alternatively, it is possible that CoRoT-7b contains a significant amount of volatiles. For a planet made of an Earth-like interior and an outer volatile-rich vapor envelope, an equally good fit to the measured mass and radius is found for a mass of the vapor envelope equal to 3% (and up to 10% at most) of the planetary mass. Because of its intense irradiation and small size, we determine that the planet cannot possess an envelope of hydrogen and helium of more than 1/10,000 of its total mass. We show that a relatively significant mass loss $\sim 10^{11} \text{ g s}^{-1}$ is to be expected and that it should prevail independently of the planet’s composition. This is because the hydrodynamical escape rate is independent of the mean molecular mass of the atmosphere, and because given the intense irradiation, even a bare rocky planet would be expected to possess an equilibrium vapor atmosphere thick enough to capture stellar UV photons. Clearly, this escape rate rules out the possibility that a hydrogen-helium envelope is present as it would escape in only ~ 1 Ma. A water vapor atmosphere would escape in ~ 1 Ga, indicating that this is a plausible scenario. The origin of CoRoT-7b cannot be inferred from the present observations: It may have always had a rocky composition; it may be the remnant of a Uranus-like ice giant, or a gas giant with a small core that would have been stripped of its gaseous envelope.

Conclusions. With high enough sensitivity, spectroscopic transit observations of CoRoT-7 should constrain the composition of the evaporating flow and therefore allow distinguishing between a rocky planet and a volatile-rich vapor planet. In addition, the theoretical tools developed in this study are applicable to any short-period transiting super-Earth and will be important to understanding their origins.

Key words. (Stars:) planetary systems, (Stars:) planetary systems: formation, Stars: individual: CoRoT-7

1. Introduction

The newest planet discovered by space mission CoRoT is remarkably interesting. CoRoT-7b is not only the first super-Earth with a measured radius, but orbits extremely close to its parent star, only 4.27 stellar radii away (Leger et al., 2009). Its radius, and orbital period are $R = 1.68 \pm 0.09 R_{\oplus}$, and $P = 0.854$ days respectively, the calculated age and equilibrium temperature are $\sim 1.2\text{--}2.3$ Ga and 1800–2600 K (Leger et al., 2009) respectively, and the mass reported by radial velocity measurements is $M = 4.8 \pm 0.8 M_{\oplus}$ (Queloz et al., 2009).

While the combination of mass (M) and radius (R) measurements alone does not yield a unique solution for the composition of a planet (Valencia et al., 2007b; Adams et al., 2008), the short period of CoRoT-7b and consequently the strong irradiation on the planet, may help constrain its composition. In this paper, we use structure models and atmospheric evaporation scenarios to investigate the physical

nature and possible origin of CoRoT-7b. We start by considering the fate of an atmosphere (section 2), before turning to the planet’s structure. Despite the intrinsic problem of degeneracy in composition, we can establish if a planet is too large to be only rocky (its radius is larger than the maximum size of a coreless magnesium-silicate planet), or even too large to be icy (its radius is larger than the maximum size of a snowball planet) given its mass. We describe the model used to calculate the planet’s structure (section 3), and show that for a subset of radius-mass combinations within the data, CoRoT-7b would in fact be too large to be composed of only refractory material. We present our results on the composition of CoRoT-7b and discuss possible evolution scenarios including as an evaporated ice or gas giant planet (section 4). We conclude by providing arguments for the most likely scenario for CoRoT-7b.

The framework presented here is applicable to any transiting close-in super-Earth. Moreover, owing to the bias

of discovering short-period planets, we expect many such super-Earths to be discovered in the near future with the next phases of CoRoT and Kepler's observations.

2. Mass Loss

Close-in planets are vulnerable to evaporation because of intense irradiation from their parent star. Indeed, gas has been detected to flow out from the transiting gas giant HD 209458b (Vidal-Madjar et al., 2003). Certainly, CoRoT-7b, whose mean density is 4–8 g cm⁻³ is denser than HD 209458b ($\bar{\rho} = 0.33$ g cm⁻³) by at least an order of magnitude. However, the UV flux received by CoRoT-7b is greater by an order of magnitude, because it is closer to its parent star and somewhat younger compared to HD 209458b (0.017 AU and 1.2–2.3 Ga compared to 0.047 AU and \sim 4 Ga). One could therefore expect mass loss rates that are comparable within an order of magnitude for the two planets. Consequently, given that CoRoT-7b is 40 to 55 times less massive than HD 209458b, this mass loss may have a profound effect on its evolution, fate and present composition. We now attempt to quantify this mass loss, using simple assumptions (the precise modelling of atmospheric escape in this planet is a difficult task beyond the scope of this article).

We model the atmospheric escape using the well-known expression for the extreme case of energy-limited escape, the validity of which has been verified for gas-giant planets close to their star (see review by Yelle et al., 2008):

$$\dot{M}_{\text{esc}} = \frac{3\epsilon F_{\text{EUV}}}{4G\bar{\rho}_p K_{\text{tide}}}, \quad (1)$$

where F_{EUV} is the incident flux of the stellar EUV (extreme ultraviolet radiation), ϵ is the heating efficiency defined as the ratio of the net heating rate to the rate of stellar energy absorption, $\bar{\rho}_p$ is the mean density of the planet, K_{tide} is a correction factor to include the Roche-lobe effect (Erkaev et al., 2007; Lecavelier des Etangs et al., 2004), and G is Newton's constant. Of course, most of the physics is hidden in the parameter ϵ which is mainly controlled by the ability of the upper atmosphere to cool. In the case of close-in gas giants, detailed calculations show that H_3^+ plays a dominant role for the cooling of the upper atmosphere. In particular, Eq. (1) with $\epsilon = 0.4$ and HD 209458b's characteristic values yields $\dot{M}_{\text{esc}} = 4 \times 10^{10}$ g s⁻¹, which is to be compared to values between 3.5 and 4.8×10^{10} g s⁻¹ obtained in the literature (Yelle et al., 2008, and references therein).

For planets with different atmospheric compositions, one may question the validity of the relation. Tian et al. (2008) have recently simulated the escape of the Earth's atmosphere for different EUV irradiation levels. They demonstrate that, for EUV irradiation fluxes above \sim 10 times the solar value, the atmosphere is in the hydrodynamic regime, namely that it escapes in an energy-limited fashion rather than through blow-off or in a diffusion-limited way. While thermal conduction is important for moderate EUV fluxes, implying that mass loss then depends on atmospheric composition, its contribution is found to become negligible for strong EUV fluxes—as it is in our case—. This can also be seen by the fact that the ratio of the EUV flux that the planet receives to a typical energy flux due to thermal conduction is $\beta \approx 10^{10-11}$, and that the ratio of a typical energy flux to a thermal conduction flux is $\zeta \approx 10^{3-5}$,

provided that the thermal conduction coefficient is of the same order of magnitude as that for hydrogen molecules (see García Muñoz (2007), for a similar discussion about HD209458 b, and Watson et al. (1981) for a precise definition of β and ζ).

As described above, the escape efficiency is controlled by the radiative cooling by H_3^+ in the case of hydrogen atmospheres. In the case of water-rich atmospheres, oxygen from dissociation of H_2O prevents a significant amount of H_3^+ from forming, which means the efficiency might be higher (e.g., García Muñoz, 2007). Indeed, for the case of the Earth the values of the exobase temperature and velocity of Fig. 8 of Tian et al. (2008), one obtains the mass loss rate of the order of 10^9 g/s in the case of the highest EUV flux ($= 100$ erg s⁻¹ cm⁻²), while Eq. (1) yields for the same conditions $\dot{M}_{\text{esc}} \sim 10^9$ g/s. For silicate atmospheres, no calculations exist, but we can presume that in the likely absence of species that cool much more efficiently than H_3^+ , Eq. (1) with $\epsilon = 0.4$ should remain valid within an order of magnitude—we will come back to this particular case in §4.1.3. In conclusion, *mass loss should remain relatively large whatever the properties of the atmosphere (and its mean molecular weight)*.

Another important quantity controlling the escape flux is the flux of EUV photons emitted by the star, which is strongly dependent on the stellar age:

$$F_{\text{EUV}} = \alpha t_9^{-\beta} a_1^{-2}, \quad (2)$$

according to recent observations of EUV emission from young stars (Ribas et al., 2005); where t_9 is the stellar age in Ga, a_1 the planet's orbital distance in AU, and α and β are constants. Their best-fit result for Sun-like stars similar to CoRoT-7 is obtained with $\alpha = 29.7$ erg s⁻¹ cm⁻² ($\equiv \alpha_{\text{R05}}$) and $\beta = 1.23$. With this expression and values, one obtains that $F_{\text{EUV}} = 5.0 \times 10^4$ erg s⁻¹ cm⁻² for CoRoT-7b ($t_9 = 1.8$ and $a_1 = 0.017$), while 2.4×10^3 erg s⁻¹ cm⁻² for HD209458 b ($t_9 = 4.0$ and $a_1 = 0.047$).

It can be noted that with such a high UV irradiation flux, CoRoT-7b may be above the purely energy-limited escape regime and in a regime limited by the recombination of electrons and hydrogen nuclei, implying $\dot{M}_{\text{esc}} \propto (F_{\text{EUV}})^{0.6}$ (Murray-Clay et al., 2009). This would imply mass loss rates about twice lower than estimated here with $\epsilon = 0.4$ and eq. (1). As we are concerned with orders of magnitude estimates, this possibility will be ignored in the rest of the work.

Using values characteristic of CoRoT-7b in Eq. (1), one obtains

$$\dot{M}_{\text{esc}} = 1 \times 10^{11} t_9^{-\beta} f_{\text{esc}} \text{ g s}^{-1} \quad (3)$$

with

$$f_{\text{esc}} = \left(\frac{\alpha}{\alpha_{\text{R05}}} \right) \left(\frac{a_1}{0.017} \right)^{-2} \left(\frac{\epsilon}{0.4} \right) \left(\frac{\bar{\rho}_p}{\bar{\rho}_{\oplus}} \right)^{-1} \left(\frac{K_{\text{tide}}}{0.65} \right)^{-1}. \quad (4)$$

With the reported age of CoRoT-7b, $t_9 = 1.2$ – 2.3 (Leger et al., 2009), and $\beta = 1.23$, Eq. (3) yields values for the escape rate, $\dot{M}_{\text{esc}} = (5$ – $10) \times 10^{10}$ g s⁻¹, similar to that for HD209458 b.

To obtain the total mass lost before t_9 , we integrate eq. (1), so that

$$M_{\text{esc}} = 0.7 \left(\frac{t_9^{1-\beta} - t_{9,0}^{1-\beta}}{1-\beta} + t_{9,0}^{1-\beta} \right) f_{\text{esc}} M_{\oplus}, \quad (5)$$

where $t_{9,0}$ is the time during which the EUV flux is constant and taken to be 0.1. Using eq.(5) with $\epsilon = 0.4$, assuming a planet density that is constant in time and CoRoT-7b's characteristic values, one obtains a cumulative escaped mass that goes from $\sim 2.3 M_{\oplus}$ for a $5.8 M_{\oplus}$ planet to $\sim 4.5 M_{\oplus}$ for a $4 M_{\oplus}$ planet. Hence, CoRoT-7b's present mass is in agreement with a planet that has not lost much more than half its initial mass. However, this picture can be significantly modified when the planet's density varies greatly with time, namely, in the case of planets with vapor or hydrogen envelopes, as we will see in §4.2.5.

Without a detailed calculation of heating and cooling effects which depend on the exact composition of the escaping atmosphere, this should be considered only as an order of magnitude estimate. However, it shows that for any atmosphere to be present, it must constantly be resupplied and that the planet may have already lost a significant fraction of its mass. On the other hand, this does not mean that this planet happened to be detected on its way to complete evaporation. By integrating eq. (3), one finds that the current state is rather stable, mainly because of the weakened EUV; complete evaporation takes more than 10 Ga for $\epsilon = 0.4$.

In any case, our estimates leave room for a rather large ensemble of possibilities concerning the global composition of the planet: it may possess iron and rocks but also volatiles or even hydrogen and helium, and the question of how much of these may be present arises. We attempt to address this in the following sections.

3. Modelling interior structure and evolution

3.1. Procedure

In order to calculate the possible structure and evolution of Earth-like planets up to ice giants and gas giants, we combine two models. For the solid/liquid regions we use a 3 layer (iron/rock/ice) hydrostatic model based on Vinet and shock equations of states; each layer is assumed to be isentropic except for the conductive thermal boundary layers at the top and bottom of the mantle (Valencia et al., 2006, 2007b). This model reproduces the Earth's structure well and has been used previously to understand super-Earths properties. For gaseous/fluid envelopes, we use a quasi-static model of interior structure and evolution that has been extensively used to model solar and extrasolar giant planets (Guillot & Morel, 1995; Guillot, 2005). The two models are tied by using the pressure at the bottom of the gaseous/fluid envelope as an upper boundary condition for the calculation of the structure of the solid/liquid interior. The temperature is *not* consistently calculated between the two models. However, this should not affect the results because thermal effects have a negligible impact on the properties of high-pressure iron, rocks and solid ices.

Our purpose is to understand possible compositions of CoRoT-7b. The thermal evolution of such a planet is uncertain because it depends on its composition, initial state,

dynamical evolution, all of which are unknown. It also depends on atmospheric properties and opacities, two quantities that are difficult to estimate for a planet that probably has a very different atmospheric composition from what has been usually considered. Fortunately, those two quantities give small impacts on our results, as described below. Following Guillot (2005), evolution calculations are obtained using a simplified atmospheric boundary condition

$$T_{10} = T_{0*} (1 + L/L_{\text{eq}})^{1/4}, \quad (6)$$

where T_{10} is the temperature at the 10 bar level, L is the planet's intrinsic luminosity, L_{eq} corresponds to the stellar luminosity that it receives and T_{0*} is chosen equal to 2500 K to account for the presence of a greenhouse effect similar to what is obtained for the atmospheres of close-in giant exoplanets (e.g. Iro et al., 2005). In fact, because the thermal evolution of highly irradiated planets is rapidly governed by the growth of an inner radiative zone, it is weakly dependent on the choice of the outer boundary condition. What is most important to us is that the high (~ 2000 K) irradiation temperatures of CoRoT-7b maintain the atmosphere well above the condensation temperature of water, so that a vapor atmosphere may be present for a long time. (This is contrary to planets in colder environments which require a large L to maintain photospheric water vapor, and therefore cool quickly until they become solid).

For opacities in gaseous envelopes, we use the Rosseland opacity table of Alexander & Ferguson (1994). The table is valid for a hydrogen-helium solar composition mixture so that its application to other atmospheres (e.g. one mainly formed with water vapor) may be questioned. We point out however that the cooling is generally controlled by the opacity in a region at a pressure $P \sim 1 - 10$ kbar and $T \sim 3000$ K, for which the opacities are extremely uncertain, regardless of the assumed composition (Guillot et al., 1994). At these pressures and temperatures, it is mostly controlled by collision-induced absorption by molecules in the infrared, and by the presence of electrons that yield important absorption (e.g. from H^- for a hydrogen rich gas) at visible wavelengths. As a result, the opacities increase rapidly with increasing P and T , whatever the assumed composition. The switch from an almost isothermal external layer to a nearly adiabatic envelope in deeper regions is expected to occur abruptly. In this case also, the quantitative uncertainties on the underlying physical parameters are large, but they have a limited impact on the result, and they do not change qualitatively our conclusions.

Finally, the boundary condition at the bottom of the envelope is defined as a radius provided by the hydrostatic model of the solid/liquid interior, and a luminosity:

$$L_0 = \dot{\epsilon}_{\text{radioactive}} M_{\text{R}} + C_V \frac{dT_{\text{Fe+R}}}{dt} M_{\text{Fe+R}}, \quad (7)$$

where $\dot{\epsilon}_{\text{radioactive}}$ is the radioactive luminosity per unit mass, M_{R} is the mass of the (rocky) mantle, C_V is the rock + iron core specific heat, and $T_{\text{Fe+R}}$ is a characteristic temperature of the solid region of mass $M_{\text{Fe+R}}$. In the calculations, we assume a chondritic value $\dot{\epsilon}_{\text{radioactive}} = 2 \times 10^{20} \text{ erg s}^{-1} M_{\oplus}^{-1}$, $C_V = 10^7 \text{ erg g}^{-1} \text{ K}^{-1}$ and $dT_{\text{Fe+R}}/dt = dT_{\text{env}}/dt$, where T_{env} is the temperature at the bottom of the envelope. However, we found results to be quite insensitive to the choice of the inner boundary condition because

for most cases, L was found to be significantly larger than L_0 .

3.2. States of matter inside CoRoT-7b

We now describe the different phases and states of matter for a generic super-Earth given all possible compositions and emphasize the relevant structure for a short-period planet like CoRoT-7b.

3.2.1. Hydrogen and helium

In Uranus and Neptune, hydrogen and helium form about 1 to 4 M_{\oplus} of the planets' outer envelopes (e.g Guillot, 2005, and references therein). While it is not necessary expected in a planet as small in size as CoRoT-7b, it is interesting to consider them and provide upper limits to their abundances in the planet.

Of course, given the temperatures to be considered (~ 2000 K and above) and pressures well below a Mbar, hydrogen and helium are expected to behave as a gas with hydrogen in molecular form (see phase diagram in Guillot, 2005). The equation of state considered for modeling their behavior is that of Saumon et al. (1995).

3.2.2. Water and “volatiles”

Because of their large abundances, moderately refractory species such as water, methane, ammonia are crucial building blocks of planetary systems. They are often grouped within the denomination of “ices” in the literature. In order to avoid the confusion with solid water, we prefer to call them “volatiles” and will use this term throughout the rest of the article. In a primordial disk with near-solar composition and temperatures below ~ 200 K, volatiles are by far the dominant solid species to condense (Barshay & Lewis, 1976). Among those, water dominates, first because oxygen is more abundant, and second because water condenses at higher temperatures than ammonia and methane. In a solar composition mixture, oxygen is more abundant than carbon by a factor 1.8, to nitrogen by a factor 7.2 and to magnesium, silicon and iron by factors 12, 15 and 15, respectively (Asplund et al., 2009). We hereafter use water as a proxy for volatiles in general, an assumption that is minor compared to other sources of uncertainty.

From the phase diagram of H_2O (Fig. 1) it is clear that with an atmospheric temperature above 1000 K, the planet would be composed of supercritical water. If the planet follows an adiabat, it will remain in vapor form transforming eventually into a plasma. If instead, the planet had a surface temperature below the melting point of water (e.g. because it formed far from the central star), it would exhibit different high pressures forms of ice, up to a regime where ice VII and ice X (for the massive icy planets) dominate.

The EOS used for water vapor is obtained from a combination of data obtained from a finite temperature molecular dynamics (FT-DFT-MD) simulation by French et al. (2009) and of the Sesame 7150 EOS (see Kerley 1972). The FT-DFT-MD data are used for $T = 1000 - 10,000$ K and $\rho = 2 - 7 \text{ g cm}^{-3}$ as well as for $T = 10,000 - 40,000$ K and $\rho = 5 - 15 \text{ g cm}^{-3}$. Sesame 7150 data are used elsewhere. The two EOS are joined by interpolation of isotherms.

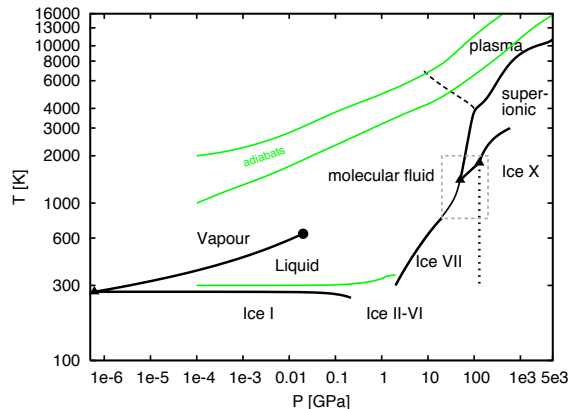


Fig. 1. Phase diagram of water from 0.01 bar to 50 Mbar and 300 to 16000 K. *Black solid lines*: phase-transition boundaries, *Triangles*: Triple points, *Circle*: critical point; *grey solid lines*: adiabats starting from 300, 1000, and respectively 2000 K at 1 bar; *black dashed line*: continuous transition from molecular dissociated water to water plasma; *grey dashed box*: region of high uncertainty and contradictory experimental and theoretical results. For $P > 4$ GPa and $T \geq 1000$ this diagram relies on data from FT-DFT-MD calculations French et al. (2009). The melting curve is taken from Feistel et al. (2006), the saturation curve from Wagner & Pruß (2002), and the phase boundary of Ice VII is adapted from Goncharov et al. (2009) for pressures lower than 30 GPa. For higher pressures, experimental and theoretical investigations predict different phase boundaries Ice VII–molecular water, Ice VII–superionic water, Ice VII–Ice-X (controversial as a hard boundary from experiments (Hemley et al., 1987)), IceX–superionic water and different locations of corresponding triple points French et al. (2009); Goncharov et al. (2009); Schwager et al. (2004).

3.2.3. Silicates

Although silicates are basically made of $(Mg,Fe)O + SiO_2$, the phase diagram relevant for the mantle is very complicated due to the different minerals that can be formed and the presence of iron and other minor elements (Ca, Al). We show the relevant phases for the magnesium end member in Fig. 2. The diagram shows the forsterite (Fo: Mg_2SiO_4), perovskite/post-perovskite (pv/ppv: $MgSiO_3$), magnesiowustite (mw: MgO) system. In addition, the upper mantle would also include the pyroxene phases ($Mg_2Si_2O_6$).

We show two adiabats calculated at 300 K and 2000 K and 1 bar for comparison. Both melting curves of pv and mw show a steep slope that can pose a barrier to melting of the interior. Given that we do not know the melting behaviour of post-perovskite or of MgO at large pressures, it remains unclear if the lower-most mantle of super-Earths can easily melt or not.

It should be noted that melting will depend on the amount of iron in the mantle (i.e. the magnesium number), but also on the abundance of minor species, something not included in Fig. 2. As an example, on Earth, decom-

pression melting can occur at temperatures around 1300K (Hirschmann, 2000). We do not attempt to determine the fraction of the planet’s surface that may be molten, but note that it may be relatively large.

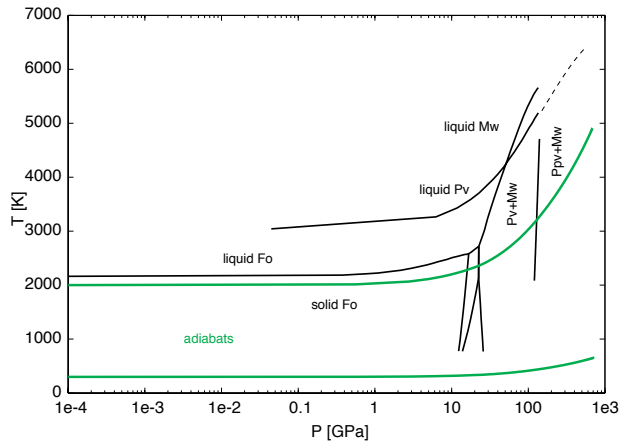


Fig. 2. Simplified $P - T$ phase diagram for relevant silicates on super-Earths. Data is taken from Presnall (1995) for the Mg-silicate end member, with phase boundaries from solid forsterite (dominant in the upper mantle), to Earth’s lower mantle materials, perovskite (pv) and magnesiowustite (mw). The melting curve for pv and mw, which remains controversial, are shown, as well as an extrapolation of the pv’s melting curve to higher pressures. The phase boundary of post-perovskite (ppv) was calculated from Tsuchiya et al. (2004). Adiabats at 300 K and 2000 K and 1 bar are shown for reference.

3.2.4. Iron

While forming a pure iron planet is very unlikely, evaporating the mantle of a Mercury-like planet might be possible. We show the phase diagram for iron in Fig. 3. Different phases of iron have been identified in the low pressure regime (Boehler, 2000) with relative agreement. The ϵ phase seems to be the most relevant to Earth’s core. A pure-iron planet might transition between different phases of iron depending on the pressure-temperature profile. However, the high pressure regime in which most of the cores of super-Earths would be in, is still inaccessible to experiments. Thus, it is unclear if there are any other higher pressure phases of iron unidentified at this point. One study (Morard et al., 2009) has reported from ab-initio calculations the melting behaviour of iron in the tens of megabars pressure regime (red and black symbols in Fig. 3). The melting boundary is quite steep implying that pure-iron planets are likely to be mostly solid. However, planets with mantles have hotter interiors due to their insulating character.

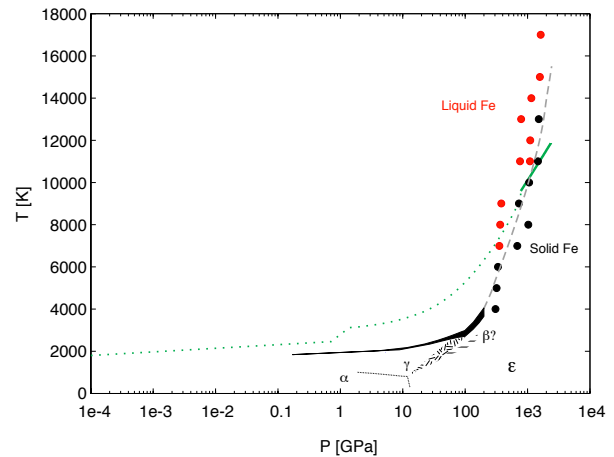


Fig. 3. $P - T$ phase diagram for iron. Values for pressures below 200 GPa were adapted from Boehler (2000) and references therein. The black region shows the agreement in the melting curve of iron at relatively low pressures. Data points for melting in the high pressure regime of 306-1625 GPa are from Morard et al. (2009). Red points correspond to the liquid phase, while black points are solid Fe. The dash curve is a melting line drawn to approximate the boundary suggested by the results from the ab-initio calculations. The temperature profile for an Earth-like CoRoT-7b is shown in green. The dotted part corresponds to the mantle, whereas the solid line corresponds to the core’s temperature.

4. Inferring Composition

4.1. CoRoT-7b as a rocky (iron+rock) planet

4.1.1. Description

We first explore the case in which the planet is of telluric composition. This implies a variety of compositions, from a pure magnesium-silicate planet (with no iron) to a pure iron planet. The former would yield the largest size for a rocky body, while the latter would be the smallest. Either case is unlikely. During the cooling of a protoplanetary disk, iron and silicates are condensed out at similar temperatures so that if iron is present, so are silicates, and viceversa, especially in large objects. Furthermore, the variety in structure for rocky planets includes those that are differentiated and undifferentiated. The former has a layered structure with the core composed mainly of iron, and in the case of Earth some nickel and a light alloy (McDonough & Sun, 1995) below a silicate mantle. The mantle can also incorporate iron within the oxide structure replacing the magnesium site. Undifferentiated planets would have all of their iron content embedded in the mantle rocks. The amount of iron with respect to magnesium in the mantle (the magnesium number) speaks to the degree of differentiation of a planet and is a consequence of early formation, when the part of Fe that remained immiscible differentiated to form the core. The iron content $x_{\text{Fe}} = \text{Fe}/(\text{Mg} + \text{Fe})$ for Earth has been estimated at 0.1 (McDonough & Sun, 1995), while for Mars it is calculated to be 0.20-0.25 (Ohtani & Kamaya, 1992). For super-Earths this number may greatly vary, although due to larger accretional energies, bigger planets may be expected to be differentiated.

On the other hand, the composition of planets can be compared by looking at bulk elemental ratios such as Fe/Si. For Earth this number is considered to agree with that of CI chondrites (McDonough & Sun, 1995) and is ~ 2 . Although it is unclear if the planets should have the same Fe/Si bulk ratio as their host star, it is a reasonable assumption. Mercury is an anomaly in the solar system. However its anomalously high iron content may be related to secondary formation processes like giant impacts and erosion, which may have dramatic effects on planetary compositions.

To infer CoRoT-7b's composition we considered different possibilities: 1) A pure Mg-silicate planet; 2) an Earth analog (i.e. a differentiated planet with $x_{\text{Fe}} = 0.1$, and a core that is 33% by mass); 3) an undifferentiated planet with the same bulk Fe/Si ratio as Earth's, which we obtain with an iron content of $x_{\text{Fe}} = 0.76$ by mol; (4) a planet with no iron in the mantle and a core-mass fraction of 63% (i.e. a super-Mercury); and (5) a pure iron planet. The mass-radius relations are shown in Figure 4.

To calculate the Fe/Si ratio of the differentiated and undifferentiated planets we considered a mantle composed of $\frac{1}{2}(\text{Mg}_{(1-x_{\text{Fe}})}, \text{Fe}_{x_{\text{Fe}}})_2\text{SiO}_4 + \frac{1}{2}(\text{Mg}_{(1-x_{\text{Fe}})}, \text{Fe}_{x_{\text{Fe}}})_2\text{Si}_2\text{O}_6$ in the upper mantle and $\frac{3}{4}(\text{Mg}_{(1-x_{\text{Fe}})}, \text{Fe}_{x_{\text{Fe}}})\text{SiO}_3 + \frac{1}{4}(\text{Mg}_{(1-x_{\text{Fe}})}, \text{Fe}_{x_{\text{Fe}}})\text{O}$, in the lower mantle and lowermost mantle (the post-perovskite region). In addition, we used a Ni/Fe ratio of 17 and had a light alloy in the core of 8% by mass after Earth's composition (McDonough & Sun, 1995).

Owing to the fact that the largest radius for a rocky CoRoT-7b corresponds to the Mg-silicate planet, any radius above this line reveals the presence of volatiles. Rocky planets with increasing amounts of iron content, whether differentiated or undifferentiated will have a mass-radius relation lying progressively below the pure Mg-silicate line. Coincidentally, this 'super-Moon' composition conforms to the smallest and largest mass of CoRoT-7b. However, it is unrealistic as iron is expected to be present in some amount, so that the lower end of CoRoT-7b's mass range can not be justified without the presence of volatiles. Massive planets mostly made of silicates and with very little iron ("super-Moons") are unlikely to exist: it is difficult to imagine how the special conditions that led to the formation of our Moon could also prevail for a planet 500 times more massive, and with the disappearance of the massive iron-rich counterpart object (equivalent to the Earth).

The difference between differentiated and undifferentiated planets is that the latter are slightly larger and this effect becomes more noticeable with increasing mass. Our result agrees with that of Elkins-Tanton and Seager (2008). The difference in radius for planets with 1, 5, 10 and 15 M_{\oplus} is of 0.7%, 1.5%, 2.6% and 3.4% respectively. Thus, from mass and radius measurements it seems implausible to distinguish between a differentiated and undifferentiated planet. However, perhaps atmospheric evaporation of silicates indicating the amount of iron might help infer the state of differentiation.

We exemplify the different structures of an Earth-like composition and the equivalent undifferentiated planet in terms of the Fe/Si. For a fixed radius of $R = 1.68 R_{\oplus}$ the differentiated and undifferentiated cases would have a mass of 5.6 and 5.3 respectively. Figure 5 depicts their different interiors.

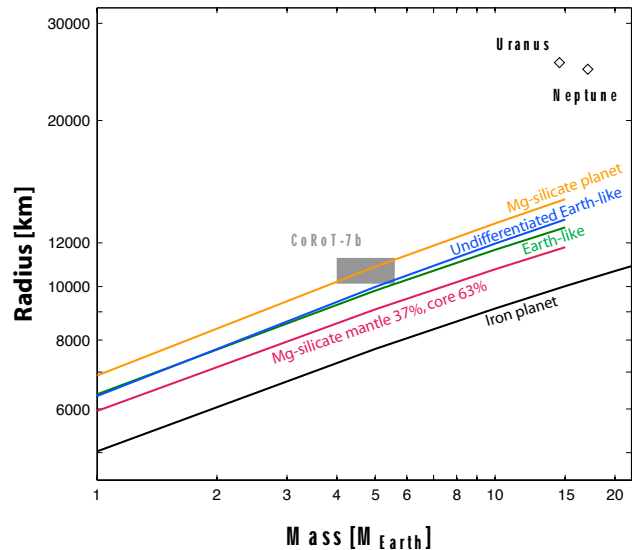


Fig. 4. Mass-radius relations for planets made of iron and rocks. The compositions considered are pure iron, 63% core and 37% mantle, Earth-like (33% core and 67% mantle with $x_{\text{Fe}}=0.1$ iron content), an undifferentiated planet with bulk Fe/Si=2 (Earth-like), and 100% Mg-silicate mantle planet. The surface temperature is taken to be 1800 K. The shaded area corresponds to CoRoT-7b's measured radius and mass. Any combination of M-R that lies above the relation for pure Mg-silicate planets (orange line), requires a composition that includes volatiles. Compositions with larger amounts of iron would progressively lie below this line.

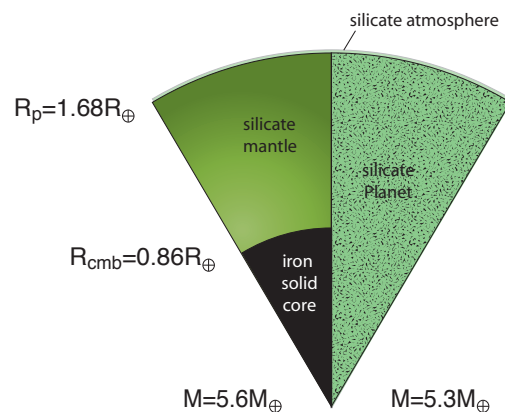


Fig. 5. Drawing to show the interior structure envisioned for a rocky planet. Two scenarios with Fe/Si = 2: (left) Earth-like (10% by mol of iron in the mantle, and core-mass fraction of 33%), or (right) undifferentiated.

Furthermore, the state of the core is shown in Fig. 3, where we show the temperature profile for an Earth-like composition including concentration of radioactive sources and an age of 1.8 Gy. The core's temperature lies right at the melting boundary, so that given the uncertainties in temperature structure there is a possibility of an outer liquid core. These uncertainties include the exact concentration of radioactive sources (perhaps more potassium),

the existence of a boundary layer right above the core, and even possibility of a layered mantle due to the different viscosities between perovskite and postperovskite. Given the very steep behavior of the iron solidus, it seems unlikely that massive terrestrial planets could have liquid cores, especially those with a surface temperature that allows for liquid water.

4.1.2. The atmosphere

Because of the large irradiation the planet is subject to, its surface may be heated to extremely high temperatures. Given the star’s characteristics ($T_{\text{eff}} = 5275 \text{ K}$, $R_{\star} = 0.87 R_{\odot}$) and planet’s semi-major axis ($a = 4.27 R_{\star}$), the effective equilibrium temperature at the planet’s substellar point is (assuming a zero albedo) $T_{\text{eq}}^{\text{sub}} = 2570 \text{ K}$. Distributed evenly on the planet’s surface, this temperature is $T_{\text{eq}}^{\text{global}} = 1820 \text{ K}$. Even though the exact temperature depends on the emissivity and albedo, it is clear that silicates (or iron if present at the surface) should be molten by the intense heat, at least on part of the planet for temperatures above 2000 K (see Figs. 2 and 3).

A first consequence of a molten surface is that volatiles should be efficiently outgassed from the planetary interior (e.g. Schaefer & Fegley, 2007). However, because the total mass of those volatiles would be as small as at most a few 10 % of the planet’s mass, this is a temporary effect and given the significant mass loss, the massive atmosphere thus formed should disappear quickly (on a timescale of $10^6 - 10^8$ yrs, based on the arguments in §2). The remaining planet should then contain only refractory material, with vapor in equilibrium with the lava, and an evolving composition as a function of the mass loss.

Specific models for the chemistry of the atmosphere of evaporating silicate super-Earths (Schaefer & Fegley, 2009) indicate that a planet such as CoRoT-7b with a composition similar to that of the bulk silicate Earth would have an equilibrium atmosphere with a pressure initially between 10^{-6} and 10^{-2} bars (corresponding to our range of extreme temperatures). The evaporating vapor atmosphere should be mainly composed of Na, then SiO, O and O₂, then Mg, as the less refractory species are progressively lost. Schaefer & Fegley (2009) find that the pressures decrease by about 1 order of magnitude when Na is lost, and then by a further 2 to 3 orders of magnitude at 90% of total erosion.

With such a thin atmosphere, the planetary radius measured from the transits can be considered as that of the solid/liquid surface of the planet.

4.1.3. Limits to the mass loss?

Compared to the arguments presented in §2, the planet’s erosion may be reduced if (i) UV photons are not fully absorbed in the atmosphere but hit the surface of the planet, or (ii) the “supply” of atmosphere is slowed by the need to deliver heat to pass the latent heat barrier.

The photoionization cross-section of atomic species such as H, O, Fe, Mg, Si is between $\sigma_{\text{UV}} \approx 10^{-19}$ and 10^{-17} cm^2 in the 10-50 eV energy range (Verner et al., 1996). The unit optical depth for UV photons corresponds to a pressure $P_{\text{UV}} = \mu m_p g / \sigma_{\text{UV}}$, where μ is the mean molecular weight of the atmosphere, m_p the proton’s mass and g the planet’s gravity. Using $g \approx 1000 \text{ cm s}^{-2}$ and $\mu \approx 10 \text{ g}$ one finds

$P_{\text{UV}} \approx 10^{-7}$ to 10^{-9} bar. (For comparison, $P_{\text{UV}} \approx 10^{-9}$ bar for gas giants – see Murray-Clay et al. (2009)).

Because those values of P_{UV} are much smaller than those of the vapor pressure estimated above, it appears that the equilibrium vapor atmosphere is able to efficiently absorb stellar UV photons that will drive the escape from the planet. Note however that the precise rate of escape depends on cooling processes and hydrodynamical modeling much beyond the scope of this work.

Let us now consider whether a bottleneck to the escape may be caused by the need to vaporize material that is initially solid or liquid. In order to do so, we balance the energy required for the sublimation at a rate \dot{M}_{sub} with the absorbed heat flux $\pi R_p^2 F_{\star}$, where F_{\star} is the stellar irradiation. Note that F_{\star} is formally the stellar flux that reaches the ground, but given the thinness of the atmosphere, this is equivalent as the irradiation flux at the top of the atmosphere. The sublimation rate can hence be written:

$$\dot{M}_{\text{sub}} = \frac{\pi R_p^2 F_{\star}}{\mathcal{L}_{\text{sub}}}, \quad (8)$$

where \mathcal{L}_{sub} is the latent heat of sublimation. Using $\mathcal{L}_{\text{sub}} \approx 10^9 - 10^{10} \text{ erg g}^{-1} \text{ K}^{-1}$ (typical for iron and silicates), we find $\dot{M}_{\text{sub}} \approx 10^{17}$ to 10^{18} g s^{-1} , i.e. at least 6 orders of magnitude larger than the mass loss we previously derived. Hence, there is no mass loss suppression due to latent heat effects.

We thus conclude that at this orbital distance, less than 5 stellar radii away from its star, the planet should be eroding even if made of the most refractory materials!

4.1.4. Evaporation of a rocky CoRoT-7b

We now investigate the possible precursors of CoRoT-7b given that its mantle is being subjected to considerable erosion. Calculations of this erosion depend on the orbital evolution of the planet, the decrease in stellar EUV flux, but mostly on the change in bulk density as layers (or perhaps selective components) of the planet are stripped away. In this section we are mostly concerned with the effect of changing density. We integrate Eq. 1 backward in time to assess the mass loss experienced and calculate the composition of the precursors. We use the internal model to obtain the planet’s structure at each time step and calculate its density. The chosen efficiency for this calculation is $\epsilon = 0.4$. We consider two present compositions: a ‘super-Moon’ and an Earth-like composition. They correspond to the lightest and densest compositions for a rocky CoRoT-7b. The results are shown in Fig. 6 and exemplify the role of changing density.

We find that small planets suffer a larger atmospheric loss, due to the inverse dependence on average density. Also, as planets lose their silicate mantles, their average density either increases (for small planets) or stays relatively constant (for massive planets) owing to a cancelling effect between a reduction in size and mass. Thus, the rate of atmospheric loss decreases through time. Assuming $\epsilon = 0.4$, we calculate the amount of mass lost to be 3-4 M_{\oplus} , so that if formed rocky, CoRoT-7b was initially a $\sim 8 M_{\oplus}$ -planet with a core that was at most 22% by mass and Fe/Si=1.28. This is probably an upper limit, given that studies of the hydrodynamic loss of a silicate-rich atmosphere have never been done and may lead to a lower ϵ value, we do not consider

probable inward migration, or uncertainties in the EUV flux.

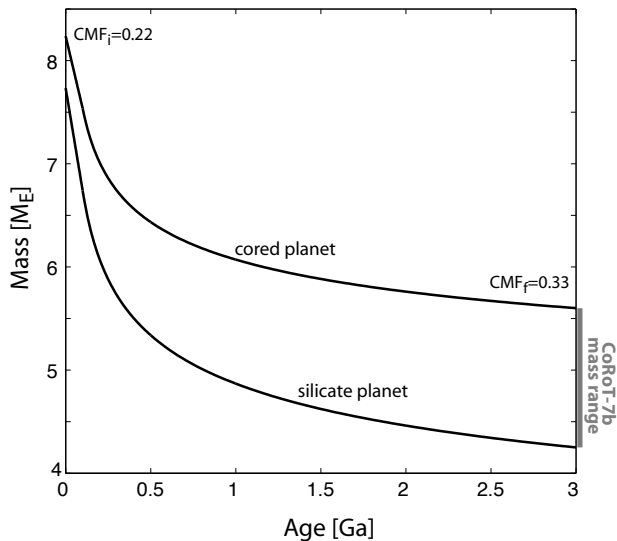


Fig. 6. Evolution in mass for CoRoT-7b for a rocky composition. Two present compositions were considered: a ‘super-Moon’ (little or no iron content), and an Earth-like composition (33% iron core, 67% silicate mantle), corresponding to the lightest and densest cases for a rocky CoRoT-7b, respectively. The initial and final proportions of core mass fraction are shown. The mass loss is more significant early on due to its inverse relation to density. The mass loss is calculated from Eq. 3, with $\epsilon = 0.4$.

4.2. CoRoT-7b as a vapor planet

4.2.1. Description and possible origin

Given CoRoT-7b’s relatively large mass, it should have originally accreted a significant mass of gases, i.e. hydrogen and helium (e.g. Ikoma & Genda (2006)), and volatiles (a.k.a “ices”) (e.g. McNeil & Nelson (2009)). Given the present extreme stellar irradiation, one would expect volatiles, if present on the planet, to be in vapor form (see §3.2). However, we first examine the alternative hypothesis that if the planet migrated from large orbital distances (e.g. Lin et al., 1996), water had time to cool and solidify.

Let us consider a planet of $M_p = 10 M_\oplus$ made mostly of water (for simplicity). The gravitational energy transformed into internal energy during its formation is $E_i \approx 3/10 GM_p^2/R_p$. In the absence of irradiation (if far enough from the star), the planet is initially made of vapor. If vapor is present in the photosphere (i.e. without an optically thick layer of hydrogen and helium), it will maintain a high atmospheric temperature (and therefore a rapid cooling) until complete condensation of water onto the interior is reached. Given an effective temperature (as obtained from the temperature at which the saturated vapor pressure (e.g. Emmanuel, 1994) is equal to the photospheric pressure, $P_{\text{vap}}(T) = 2/3 g/\kappa$), an upper limit to

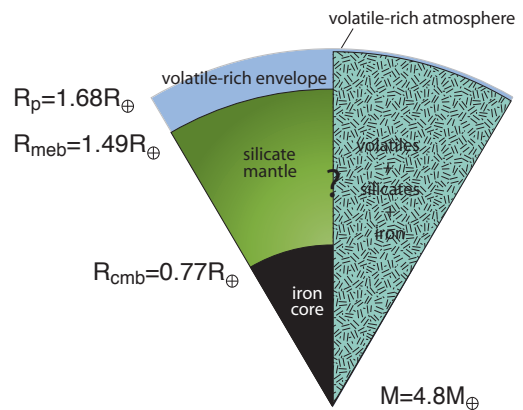


Fig. 7. Drawing to show the interior structure envisioned for a planet made of iron, rocks and volatiles in vapor form (possibly with H-He)

the time to solidification is $\tau_{\text{solid}} = E_i / (4\pi R_p^2 \sigma T_{\text{eff}}^4)$, i.e. for $R_p \approx 15,000$ km, $\tau_{\text{solid}} \approx 100$ Ma when using a low opacity $\kappa = 10^{-2} \text{ cm}^2 \text{ g}^{-1}$ ($T_{\text{eff}} \approx 320$ K). On the other hand, if ice grains and/or water droplet in the atmosphere prevent it from cooling efficiently, $\kappa \approx 10^2 \text{ cm}^2 \text{ g}^{-1}$ ($T_{\text{eff}} \approx 210$ K) so that $\tau_{\text{solid}} \approx 1$ Ga.

At least in theory, there is thus a possibility that CoRoT-7b is a planet that was formed at large distances from the star, had sufficient time (hundreds of millions of years) to solidify before being brought to an orbital distance of 0.017 AU, where ice would be sublimating again.

However, we believe that this is very unlikely for two reasons: First, a planet that massive should accrete some hydrogen and helium (Ikoma & Genda, 2006), and even only a few bars of these species would mean that water would still be in vapor form in the interior at smaller effective temperatures than estimated above in the pure water case (a situation similar to that of Uranus and Neptune). This would imply a (much) slower cooling, and thus retaining water in vapor form for a longer time. Note that invoking a putative evaporation of an outer hydrogen atmosphere would require an increased irradiation which would also be unfavorable to the rapid cooling of the planet. Second, although possibilities of slow/delayed migration exist (e.g. Wu & Murray, 2003), most of the migration scenarios require “help” from the protoplanetary disk, and therefore a migration in the first millions of years (e.g. Moorhead & Adams (2005)). In what follows, we therefore only consider the possibility that ices are in vapor form. Figure 7 depicts the two possibilities that we envision: a fully differentiated planet with iron, silicates and an extended envelope of vapor, or a fully homogeneous planet in which iron, silicates and volatiles (in vapor form) are thoroughly mixed.

4.2.2. Constraints on the presence of vapor

To estimate possible amounts of vapor compatible with the measurements of CoRoT-7b, we proceed as follows: First, for simplicity, we only consider the case of a solid/liquid interior that is “Earth-like” in composition (33% iron core, 67% mantle rock) and surrounded by an envelope of volatiles in vapor form. Our calculations of interior models

for the iron+rock part as a function of its mass $M_{\text{Fe+R}}$ and outside pressure P_0 are found to yield radii of order:

$$R_{\text{Fe+R}} = 9800 \text{ km} \left(\frac{M_{\text{Fe+R}}}{5 M_{\oplus}} \right)^{0.28+0.02\sqrt{M/5 M_{\oplus}}} \times 10^{-\left[\log_{10}(1+P_0/\sqrt{M/5 M_{\oplus}})/7 \right]^3} \quad (9)$$

where P_0 is in GPa units. The relation is an approximation found to be accurate to $\pm 0.5\%$ for $M_{\text{Fe+R}}$ between 1 and $15 M_{\oplus}$ and P_0 up to 10^3 GPa ($= 100$ Mbar). The approximation is accurate to $\pm 3\%$ to 10^4 GPa.

The size of the planet with vapor is found by calculating the evolution of an initially adiabatic planet with a specific entropy equal to that of vapor at 10 bar and 2500 K. This initial state is chosen as representative of any “hot start”, since any evolution from still higher entropies would have been fast. We neglect any possible orbital evolution of the planet.

The evolution is characterized by the rapid growth of a radiative zone just below the atmospheric boundary, similarly to what is obtained for giant exoplanets (Guillot, 2005). This zone quickly becomes isothermal and extends down to pressures around 10 kbar, and temperatures ~ 3000 K. At those pressures and temperatures, the rapid rise in radiative opacities implies that any further extension of the radiative region must wait for a large reduction of the intrinsic luminosity, implying a slow cooling. This implies that results should be relatively robust, in regard of uncertainties in initial state, opacities, age...etc.

Figure 8 shows the resulting planetary radii after 2 Ga of evolution for various mass fractions of vapor in the planet. The presence of an atmosphere of vapor is found to affect the structure and size of the planet significantly. We find that the upper limit on the amount of vapor present in CoRoT-7b is $\sim 10\%$, i.e. the equivalent to about $0.5 M_{\oplus}$. Because the cooling and contraction occurs rapidly, we find that this value is robust and doesn't change by more than a few percent when considering cooling times between 0.1 and 10 Ga. Given the evaporation rate calculated in § 2, this implies that such an atmosphere would last for another Ga or so. This is hence a reasonable possibility. Our best vapor-planet model for CoRoT-7b with a total mass of $4.8 M_{\oplus}$, has a vapor envelope that is 3% of the total mass and 12% of the total radius (see Fig. 7). For this model, the envelope is close to being isothermal: the transition between the vapor envelope and the silicate mantle is at a temperature of 2900 K for a pressure of 14 GPa.

4.2.3. Constraints on the presence of hydrogen and helium

With the same method, we derive constraints on the amounts of hydrogen and helium that may be present. Figure 9 shows that the presence of an envelope hydrogen and helium leads to a very significant increase in the size of the planet. Because of the low gravity and high compressibility of the envelope, we find that planets with smaller masses have larger radii if they contain a H-He envelope and are significantly irradiated, except when the envelope to core mass ratio is so small that the envelope is still tightly bound by gravity to the Earth-like nucleus. We derive that any hydrogen-helium envelope in CoRoT-7b must be less than 0.01% of the total planetary mass. Note that for such

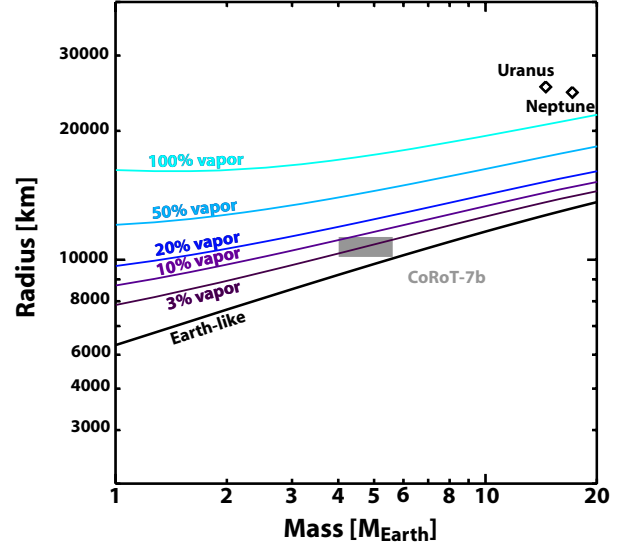


Fig. 8. Radius as a function of mass for a planet made of iron, rocks and vapor. The “Earth-like” line corresponds to the limiting value of a solid Earth-like planet with a mass fraction of iron to rocks of 33% and without vapor. Other lines correspond to radii for planets with an Earth-like interior and a vapor (H_2O) envelope, with a ratio of the mass of the vapor envelope to the total planetary mass between 3% and 100%, as labeled. The models with vapor have been evolved for 1 Ga using our fiducial opacity table (see text). Radii correspond to the 10 bar level.

small envelopes, the structure is isothermal (the envelope to silicate transition occurs at a temperature that is within a few Kelvins of the assumed 10 bar temperature). If CoRoT-7b would now possess such an envelope, it would evaporate in only 1 Ma. We therefore estimate that CoRoT-7b cannot possess a hydrogen-helium atmosphere.

4.2.4. Possibility of an undifferentiated structure

We have thus far assumed a differentiated structure (i.e., iron/rocks/volatiles or hydrogen-helium). While it is indeed verified for relatively small and cool planets (from Ganymede to the Earth), the question arises for planets that may be large and hot enough for their interior to be predominantly molten. Molten silicate and water are known to be miscible with each other at pressures above a few GPa and temperatures $> \sim 1000$ K (Shen & Kepler, 1997; Mibe et al., 2007). Above ~ 10000 K, silicate and iron are also no longer immiscible (Stevenson, 2008). Hydrogen, helium and water will also mix at high enough temperatures. Indeed, Uranus and Neptune appear to be only partially differentiated, with an outer hydrogen-helium gaseous envelope that contains a large abundance of at least one of the volatiles components, i.e. methane, an inner dense envelope which appears to be mostly made of high-pressure and high-temperature “ices”, probably mixed with rocks, and a central dense nucleus (probably made of rocks and/or iron) with a mass of order $1 M_{\oplus}$ or smaller (Hubbard et al., 1995). Some interior models compatible with the observed

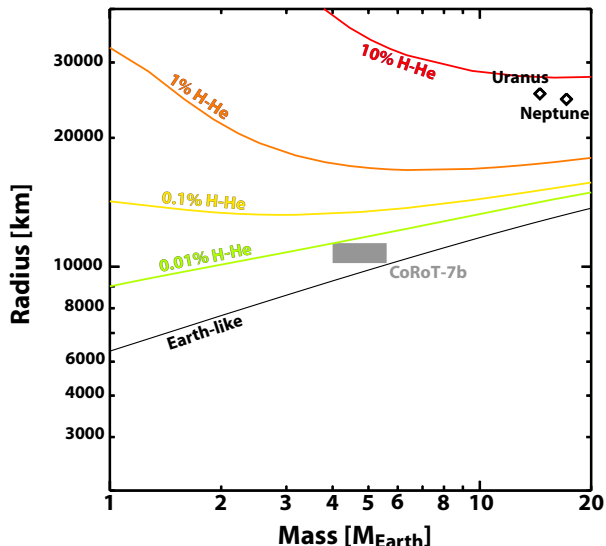


Fig. 9. Radius as a function of mass for a planet made of iron, rocks and hydrogen and helium in solar proportions. The “Earth-like” line corresponds to the limiting value of a planet without vapor. Other lines correspond to planets with hydrogen and helium envelopes having total mass fractions between 0.01% and 100% (planet made only of hydrogen and helium), as labelled. (See fig. 8).

J_2 and J_4 values even include an inner envelope composed of a mixture of hydrogen-helium and “ices” (Marley et al., 1995).

Specific studies are required to solve this problem. We stress that our limits on the presence of a gaseous or vapor envelope cannot be applied as constraints on the presence of these gases and/or volatiles in the mantle. If the planet is undifferentiated, a larger component of gases and volatiles may be present than derived in the previous sections. (This is because the higher mean molecular weight will at some point prevent the planet from inflating thermally as much as if all light species were present in an outer envelope). For robust conclusions concerning undifferentiated super-Earths in general, detailed models beyond the scope of this paper are needed. The lack of adequate equations of state and relevant opacities are difficult limitations to overcome.

In any case, we note that the mean temperature in the atmosphere should be low enough to maintain a low abundance of silicate species there. Specifically, if we assume a photospheric level close to the mean equilibrium temperature, $T_0 = 1800$ K, the saturation pressure of MgSiO_3 , representative of rock species, for that temperature is $P_s \approx \exp(-58663/T + 25.37) \approx 7 \times 10^{-4}$ bar (Lumine et al. 1987), i.e. much smaller than the photospheric pressure $P_0 = (2/3)(g/\kappa) \approx 1$ bar for $\kappa = 10^{-2} \text{ cm}^2 \text{ g}^{-1}$. We thus envision that the outer atmosphere is rich in volatiles, leading to a preferential escape of these even in the homogeneous interior case (see fig. 7).

4.2.5. CoRoT-7b as an evaporated ice or gas giant?

We now examine whether CoRoT-7b may have been formed by outstripping a gas giant or an ice giant from its envelope, leaving a planet with little or no gaseous envelope. In order to do so, we first calculate an ensemble of evolution models with a constant total mass and a constant composition. This ensemble of models is characterized by a central seed of Earth-like composition of $5 M_\oplus$ and variable total masses (from 10 to about $120 M_\oplus$). The combined mass and thermal evolution of a planet with mass loss is then calculated by noting that for each planetary mass and central specific entropy corresponds a given planetary radius, and therefore a given mass loss, and that central entropy should be conserved during mass loss:

$$\frac{dM}{dt} = f(\rho_P), \quad (10)$$

$$\frac{dS_c}{dt} = \left(\frac{\partial S_c}{\partial t} \right)_M, \quad (11)$$

where $f(\rho_P)$ is a function of the planet’s density provided by eq. 3, and the loss of central entropy S_c is calculated from individual evolution models with fixed mass.

Because evaporation is highly dependent on the planetary density, the choice of initial conditions affects the results directly. Here, we only highlight reasonable possibilities for the origin and fate of the CoRoT-7b. We assume that our planets fill their Roche lobe when formed, and allow them to contract for 10 Ma before turning on mass loss, using eq. (1). This mimics the fact that during the protoplanetary disk phase, the planet should be protected from mass loss but should have begun its contraction and loss of entropy. The result also depends on the planet’s orbital history, as a planet that is initially far from its star tends to contract faster. We therefore examine two cases: a) One in which the planet is assumed to form in situ and remain at its present orbital distance (0.017 AU) throughout its existence; b) One in which its first 10 Ma of existence are spent at larger orbital distances, i.e. ~ 0.08 AU (corresponding to an equilibrium 10 bar temperature of 1000 K), before it is suddenly brought to its present orbital distance (and an equilibrium 10 bar temperature of 2500 K).

The results are shown in Fig. 10. Vapor planets tend to be relatively compact and suffer significant but limited mass loss. For example, present observations would be compatible with a vapor planet that was initially about $12 M_\oplus$ and that lost 97% of its vapor envelope in the “in situ” case. For this type of planet, the situation remains very similar when considering the “inward migration” scenario: the additional cooling only makes the vapor envelope slightly more compact so that the “ideal” precursor mass decreases to about $10 M_\oplus$. The situation is different for hydrogen-helium planets because as was shown in fig. 9 they tend to be very tenuous and loosely bound to the rocky nucleus. For example, we find that for planets at 0.017 AU filling their Roche lobe, the evaporation proceeds faster than the contraction and always lead to the complete loss of the envelope, even for initial masses as high as the mass of Jupiter. The top panel of fig. 10 shows that even after 10 Ma of evolution without mass loss, a Jupiter-mass planet is stripped of its entire envelope in less than 80 Ma. If the planet is allowed to contract at larger orbital distances (our “inward migration” case), the resulting planet is more compact, and possible precursors to CoRoT-7b are planets less massive

than about $270 M_{\oplus}$. Thus, this shows that the evolution of layered planets maybe very different and lead to a much more significant mass loss than when considering that the planets contract with simple power laws (Lammer et al., 2009). Of course, the numbers that we derived may vary quite significantly depending on the chosen formation scenario and dynamical evolution of the planet, but at least they show that CoRoT-7b could have lost tens of Earth masses in hydrogen and helium, and that there is no impossibility that it was initially a gas giant.

teristics of CoRoT-7b: it may have been initially a gas giant planet that was eroded down to its dense rocky interior, it may have been a Uranus-like “ice giant” which would have lost most or all of its volatiles, or it may have been all the way a rocky planet with no ice or hydrogen and helium.

5. Conclusion

CoRoT-7b is the first of possibly many extreme close-in super-Earths that will be discovered in the near future. We have shown that the atmospheric escape for this type of planets is expected to be high, within an order of magnitude of that of HD 209458 b, and mostly independent of composition. A simple analysis shows that for CoRoT-7b, the mass already lost to escape would be of order $\sim 4M_{\oplus}$ for silicate-iron planets, or $\sim 10 - 100M_{\oplus}$ if the planet initially contained a massive water (hydrogen-helium) envelope.

Given the observational constraints on its size and mass, CoRoT-7b is best fitted by a rocky planet that would be significantly depleted in iron relative to the Earth. Such a massive “super-Moon” is very unlikely to form. However, a one sigma increase in mass ($5.6 M_{\oplus}$) and one sigma decrease in size ($1.59 R_{\oplus}$) would make the planet compatible with an Earth-like composition (33% iron, 67% silicates). Such a rocky planet would have a thin vapor silicate atmosphere. We estimate that this atmosphere should be thick enough to capture efficiently stellar UV photons therefore yielding a significant mass loss, possibly close to the rate obtained from energy-limiting considerations. Another possibility is that the planet was initially an ice giant that lost most of its volatile content. We calculate the maximum volatile envelope (in the form mostly of water vapor) for CoRoT-7b to be 10% by mass, with a best fit solution at 3%. We also constrain a possible hydrogen-helium outer envelope to be less than 0.01% by mass. In both cases, these numbers are derived assuming the presence of an inner rock/iron core of Earth-like composition. The precursor of such a planet may be a Uranus-like ice giant, or it may have been a more massive gaseous planet: this is because gaseous planets at very short orbital distances may be extremely extended and have their envelope only weakly bound to the central rock core. Given the fast planetary erosion, we estimate that the vapor envelope that we derive to fit the present models would last up to 1 Ga before its complete erosion. In the case of a hydrogen-helium envelope, its survival time is only 1 Ma. This therefore implies that CoRoT-7b cannot contain a hydrogen-helium envelope. It is the first time that such a conclusion can be drawn for an exoplanet. A caveat is, however, that these estimates are based on the hypothesis that the structure of the planet is in the form of distinct layers with the light species on top. It may not be the case, in particular because water and silicates appear to mix efficiently at modest temperatures and pressures (above 1000K and a few GPa), in which case potentially more volatiles may be “hidden” in the planetary interior. This is probably not a concern for hydrogen and helium because they should be mostly on top of the rocky/icy nucleous at the time of the planet formation already. With specific models, we have shown that the undifferentiation of iron with respect to silicate does not affect significantly the planetary structure either. When it comes to water and silicates, the effect may be more pronounced because of their different densities and thermal properties. Specific studies including proper equa-

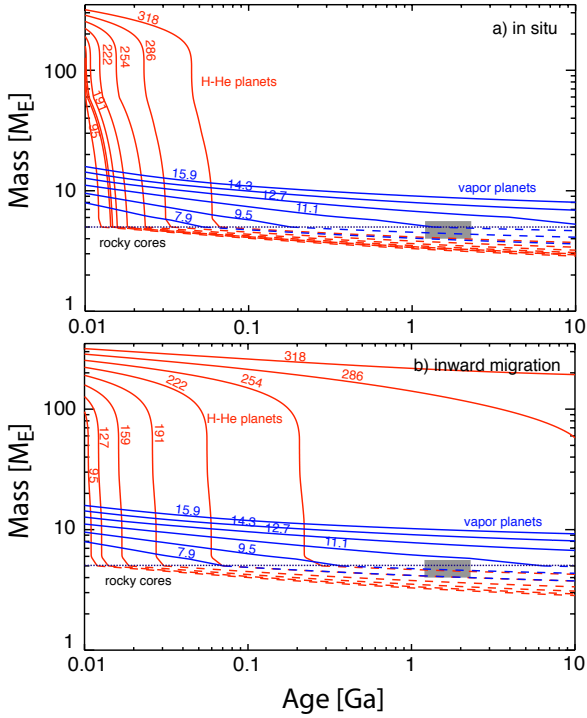


Fig. 10. Evolution of the mass of hypothetical CoRoT-7b precursors as a function of time. Two type of precursors are shown: planets with an extended hydrogen-helium envelope (red), and planets with a vapor (i.e. water) envelope. Labels indicate initial masses, in Earth masses. All cases assume an inner $5 M_{\oplus}$ Earth-like core. Plain lines indicate planets that still possess an extended envelope. Dashed lines correspond to (evaporating) bare rocky cores. The top panel assumes no migration of the planet (maximal mass-loss). The bottom panel assumes a contraction of an initially extended planet during 10 Ma at ~ 0.08 AU before migrating to its present location. The present mass and age of CoRoT-7b is indicated as a grey rectangle. A maximal, energy-limited evaporation is assumed (see text).

Our models are based on the assumption of the presence of distinct layers. An undifferentiated planet would evaporate at quantitatively different rate but we believe that qualitatively the situation would be very similar: it would lose preferentially its light elements (gases and volatiles), and at a rate that would be directly related to the proportions of hydrogen and helium and volatiles that the planet contains.

From the point of view of interior and evolution models, there is thus a range of possibilities to explain the charac-

tions of state and opacities are required to progress in that respect.

In parallel, the mass loss that we infer implies that there is a possibility to probe for the composition of the outer shell of the planet by measuring the composition of the extended planetary exosphere. CoRoT-7 ($V = 11.7$) is significantly fainter than HD209458 ($V = 7.65$), so that the measurement is challenging. However, the fact that a detection of escaping H, C and O is possible for HD 209458 b (Vidal-Madjar et al., 2003, 2004) yield great hopes for similar measurements for CoRoT-7b and close-in super-Earths in the nearby future.

Acknowledgements. This research was carried out as part of a Henri Poincare Fellow at the Observatoire de la Côte d'Azur to DV. The Henri Poincare Fellowship is funded by the CNRS-INSU, the Conseil General des Alpes-Maritimes and the Rotary International - District 1730. MI got financial support from Program for Promoting Internationalization of University Education from the Ministry of Education, Culture, Sports, Science and Technology, Japan, and from the *Plan Pluri-Formation* OPERA. The authors acknowledge CNES and the CNRS program *Origine des Planètes et de la Vie* for support. The authors further thank the CoRoT community, Guillaume Morard, Didier Saumon, Bruce Fegley and Helmut Lammer for discussions and sharing results in advance of publication, and the anonymous reviewer for helping to improve this manuscript.

References

- Adams, E., Seager, S., & Elkins-Tanton, L. 2008, ApJ, 673, 1160
 Alexander, D. R., & Ferguson, J. W. 1994, ApJ, 437, 879
 Asplund, M. N. Grevesse, A. J. Sauval, P. Scott. 2009. ARA&A
 Barshay, S. S. and J. S. Lewis. 1976. ARA&A, 14, 81
 Boehler, R. 2000, Rev. Geophys., 38, 221
 L. T. Elkins-Tanton and S. Seager. 2008, ApJ, 688, 628
 Emmanuel, K. 1994, in "Atmospheric Convection", Oxford Univ. Press, Oxford
 Erkaev, N. V., Kulikov, Y. N., Lammer, H., Selsis, F., Langmayr, D., Jaritz, G. F., & Biernat, H. K. 2007, A&A, 472, 329
 Feistel, R., Wagner, W., J. 2006, Phys. Chem. Ref. Data, 35, 1021
 Freedman, R. S., Marley, M. S., & Ladders, K. 2008, ApJS, 174, 504
 French, M., Mattsson, T.R., Nettelmann, N., & Redmer, R. 2009, Phys. Ref. B 79, 054107
 García Muñoz, A. 2007, Planet. Space Sci., 55, 1426
 Goncharov, A.F. et al. 2009, J. Chem. Phys., 130, 124514
 Guillot, T. 2005, Annual Review of Earth and Planetary Sciences, 33, 493
 Guillot, T., Gautier, D., Chabrier, G., & Mosser, B. 1994, Icarus, 112, 337
 Guillot, T., & Morel, P. 1995, A&AS, 109, 109
 Guinan, E. F., & Engle, S. G. 2009, arXiv:0901.1860
 Guinan, E. F., & Engle, S. G. 2007, arXiv:0711.1530
 Hemley, R. J., Jephcoat, A. P., Mao, H. K., Zha, C. S., Finger, L. W., & Cox, D. E. 1987, Nature, 330, 737
 Hirschmann, M. M., 2000. Mantle solidus: Experimental constraints in the effects of peridotite composition. G-cubed 1.
 Hodgkin, S. T., & Pye, J. P. 1994, MNRAS, 267, 840
 Hubbard W. B., Pearl J. C., Podolak M., Stevenson D. J. 1995. The Interior of Neptune. In *Neptune and Triton*, ed. DP Cruikshank. 109–138. Univ. of Arizona Press: Tucson
 Ikoma, M. & Genda, H. 2006, ApJ648, 696
 Iro N., Bézard B., & Guillot T. 2005, A&A, 436, 719
 Kuchner, M. J. 2003, ApJ, 596, L105
 Lakatos, S. L., Voyer, E. N., Guinan, E. F., DeWarf, L. E., Ribas, I., & Harper, G. M. 2005, Bulletin of the American Astronomical Society, 37, 442
 Lammer, H., et al. 2009, A&A, 506, 399
 Lecavelier des Etangs, A., Vidal-Madjar, A., McConnell, J. C., & Hébrard, G. 2004, A&A, 418, L1
 Leger, A., Rouan, D., Schneider, R. et al. 2009, A&A, submitted
 Lin, J., Gregoryanz, E. Struzhkin, V. 2005, GRL, 32, 11306
 Lecavelier Des Etangs, A. 2007, A&A, 461, 1185
 Lin, D. N. C., Bodenheimer, P., & Richardson, D. C. 1996, Nature, 380, 606
 Marley, M. S., Gómez, P., & Podolak, M. 1995, J. Geophys. Res., 100, 23349
 McDonough, W. F. & S.-s. Sun. 1995, Chem. Geol., 120, 223
 McNeil, D. S., R. P. Nelson. 2009. arXiv:0910.5299
 Mibe, K., Kanzaki, M., Kawamoto, T., Matsukage, K. N., Fei, Y., & Ono, S. 2007, J. Geophys. Res., 112, B03201
 Moorhead, A. V., F. C., Adams. 2005. Icarus, 178, 517
 Morard, G., Guyot F., Bouchet J., & Mazevet S. 2009, EPSL, submitted
 Murray-Clay, R. A., Chiang, E. I., & Murray, N. 2009, ApJ, 693, 23
 Ohtani, E., N. Kamaya. 1992. GRL, 19, 2239
 Penz, T., et al. 2008, Planet. Space Sci., 56, 1260
 Podolak, M., Pollack, J. B., & Reynolds, R. T. 1988, Icarus, 73, 163
 Presnall, D. C., 1994, Phase Diagram of Earth-Forming Minerals, in Mineral Physics and Crystallography A Handbook of Physical Constants, ed. Ahrens, T. J. (AGU), 354
 D. Queloz, F. Bouchy, C. Motou, A. Hatzes, G. Hebrard, R. Alonso, M. Auvergne, A. Baglin, M. Barbieri, P. Barge, W. Benz, P. Borde, H. J. Deeg, M. Deleuil, R. Dvorak, A. Erikson, S. Ferraz-Mello, M. Fridlund, D. Gandolfi, M. Gillon, E. Guenther, T. Guillot, L. Jorda, M. Hartmann, H. Lammer, A. Leger, A. Llebaria, C. Lovis, P. Magain, M. Mayor, T. Mazeh, M. Olivier, M. Patzold, F. Pepe, H. Rauer, D. Rouan, J. Schneider, D. Segransan, S. Udry, G. Wuchterl. A&A, 506: 303–, 2009.
 Ribas, I., Guinan, E. F., Güdel, M., & Audard, M. 2005, ApJ, 622, 680
 Saumon, D., Chabrier, G., & van Horn, H. M. 1995, ApJS, 99, 713
 Schaefer, L., & Fegley, B. 2007, Icarus, 186, 462
 Schaefer, L., & Fegley, B. 2009, submitted to ApJL [astro-ph:0906.1204]
 Schwager, B., Chudinovskikh, L., Gavriluk, A. & Boehler, R. 2004, J. Phys.: Condensed Matter, 16, 1177
 Schwegler, E., Sharma, M., Gygi, F., & Gallir, G. 2008, PNAS, 105, 14779
 Shen, A. H., & Kepler, H. 1997, Nature, 385, 710
 Stevenson, D. J. 2008. Nature, 451, 261
 Tian, F., Kasting, J. F., Liu, H.-L., & Roble, R. G. 2008, Journal of Geophysical Research (Planets), 113, 5008
 Tsuchiya, T., Jun, T., Kiochiro, U., & Renata, M., W. 2004, Earth Planet. Sci. Lett., 224, 241
 Uchida, T., Wang, Y., Rivers, M. L., & Sutton, S. R. 2001, J. Geophys. Res., 106, 21799
 Valencia, D., O'Connell, R. J., & Sasselov, D. D. 2006, Icarus, 181, 545
 Valencia, D., Sasselov, D. D., & O'Connell, R. J. 2007a, ApJ, 656, 545
 Valencia, D., Sasselov, D. D., & O'Connell, R. J. 2007b, ApJ, 665, 1413
 Verner, D. A., Ferland, G. J., Korista, K. T., & Yakovlev, D. G. 1996, ApJ, 465, 487
 Vidal-Madjar, A., Lecavelier des Etangs, A., Désert, J.-M., Ballester, G. E., Ferlet, R., Hébrard, G., & Mayor, M. 2003, Nature, 422, 143
 Vidal-Madjar, A., et al. 2004, ApJ, 604, L69
 Wagner, W., Pruß, A. 2002, J. Phys. Chem. Ref. Data, 31, 387
 Watson, A. J., Donahue, T. M., & Walker, J. C. G. 1981, Icarus, 48, 150
 Wu, Y., & Murray, N. 2003, ApJ, 589, 605
 Yelle, R., Lammer, H., & Ip, W.-H. 2008, Space Science Reviews, 139, 437